

Coverage Analysis of Physical Layer Network Coding in Massive MIMO Systems

Mert İlğüy , Berna Özbek , Rao Mumtaz, Sherif A. Busari , *Member, IEEE*, and Jonathan Gonzalez

Abstract—Wireless networks are prone to interference due to their broadcast nature. In the design of most of the traditional networks, this broadcast nature is perceived as a performance-degrading factor. However, Physical Layer Network Coding (PNC) exploits this broadcast nature by enabling simultaneous transmissions from different sources and thereby enhances the performance of the wireless networks with respect to improvement in spectral efficiency, coverage, latency and security of the system. For fifth generation (5G) networks and beyond, massive multiple input multiple output (MIMO) is considered as a key physical layer technology. Thus, its combination with PNC can significantly enhance the performance of the network, facilitating capacity-coverage improvement, among other benefits. While the bit error rate performance of multiuser massive MIMO-PNC systems through linear detection has been investigated extensively, their coverage probability for a given target signal-to-noise ratio has not been explored yet. In this paper, we derive a closed form expression for coverage probability in PNC based multiuser massive MIMO systems employing zero-forcing equalization. Both theoretical and simulation results are provided for different number of users and antennas in the multiuser massive MIMO-PNC communications systems.

Index Terms—Physical layer network coding (PNC), massive MIMO, multiuser systems, coverage probability.

I. INTRODUCTION

PHYSICAL Layer Network Coding (PNC) is one of the promising direction for 5G and beyond wireless networks [1]. PNC has been mainly considered for two-way relay channels (2-WRC) following Shannon's two-way channels (2-WC) [2], [3]. The 2-WC consists of two terminal nodes that want to exchange their data simultaneously. In this scenario, the transmitted signals from two terminal nodes interfere with each other. For the case in which two terminal nodes are far away from each other, an intermediate node (i.e., a relay) is needed to increase the coverage. The use of relay facilitates lower power consumption by dividing the total distance into smaller distances

for node to node transmissions. Thus, the unwanted effect of interference from other transmissions can be mitigated, leading to higher capacity per unit area.

The 2-WRC can be seen as a 2-WC with an intermediate relay node. The overall transmission is divided into two phases. The signal transmission from the terminal nodes to the relay node is the multiple access channel (MAC) phase while the signal transmission from the relay to the terminal nodes is the broadcast channel (BC) phase. As a simple scenario for wireless communication, two-terminal nodes can be considered as user equipments (UEs) while the relay can be considered as the base station (BS). In this case, the uplink corresponds to the MAC phase and the downlink corresponds to the BC phase.

Three different approaches for data exchange between two terminal nodes have been explored [2]. The first approach divides the transmission into four-time slots. In the first time slot, the first terminal node sends its data to the relay and in the second time slot, the relay just amplifies and forwards the coming data to the second terminal node. In the third time slot, the second terminal node sends its data to the relay and then in the fourth time slot, the relay amplifies and forwards the data to the first terminal node. This is the first consideration of how the terminal nodes exchange their data. However, this approach is not spectrum-efficient as it requires four orthogonal time slots for the data exchange.

In order to increase the spectral efficiency, an alternative method referred to as network coding (NC) has been examined. For this second approach, the first terminal sends its data and the relay detects and stores the bits coming from the first node in the first time slot. Then, in the second time slot, the second terminal node sends its data to the relay which detects and stores the bits. In the third time slot, the relay performs pairwise exclusive OR (XOR) operation of the stored bits and broadcasts the network-coded data to the two terminal nodes. Since the terminal nodes know their data, they can extract the data of the other node through the XOR operation.

The third approach which is PNC allows two simultaneous transmissions in the same time slot. Here, the first and second terminal nodes simultaneously transmit their signals in the first time slot. Then, the relay receives the combined signal and decides the suitable network coded symbol (NCS) according to the optimal network coding operation which allows unambiguous decoding at the terminal nodes. The relay then broadcasts the network-coded data back to the terminals in the second time slot, thereby reducing the total number of needed orthogonal time slots to only two. For the binary case, the optimal operation is XOR. At the MAC phase, the difference between NC and PNC

Manuscript received July 6, 2020; revised November 27, 2020; accepted January 3, 2021. Date of publication January 21, 2021; date of current version March 10, 2021. This work was supported by the European Union Horizon 2020, RISE 2018 Scheme (H2020-MSCA-RISE-2018) under the Marie Skłodowska-Curie Grant Agreement 823903 (RECENT). The review of this article was coordinated by Prof. X. Wang. (*Corresponding author: Berna Özbek.*)

Mert İlğüy and Berna Özbek are with the Electrical, and Electronics Engineering Department, Izmir Institute of Technology, Izmir 35430, Turkey (e-mail: mertilguy@iyte.edu.tr; bernaozbek@iyte.edu.tr).

Rao Mumtaz, Sherif A. Busari, and Jonathan Gonzalez are with the GS-Lda, Águeda 3750-101, Portugal (e-mail: shmu@gs-lda.com; sbusari@gs-lda.com; jonathan@gs-lda.com).

Digital Object Identifier 10.1109/TVT.2021.3053294

is that PNC maps directly the received constellation points to their corresponding NCSs without applying the bitwise network coding operation while NC separately detects the users' data in different time slots to perform their bit-wise network coding operation. The BC phase is the same for both NC and PNC [2].

In the literature, the performance evaluation of PNC has been considering mostly based on the capacity and bit-error-rate (BER) metrics. In [3], the concept of PNC has been given in terms of sum capacity while the BER performance of PNC have been compared to the conventional and NC based transmission schemes when the terminal nodes have different signal-to-noise ratio (SNR) in [4]. Since the PNC based scheme decides the suitable NCS according to the received constellation, its performance highly depends on the modulation type. In [5]–[7], the authors examined the performances of PNC over different modulation schemes such as QPSK, M-PSK and M-QAM based on closed form BER expressions.

The massive multiple input multiple output (MIMO) is one of the promising technologies for the wireless communication systems. The combination of massive MIMO and PNC can significantly increase the overall network performance. For the PNC with multiple antennas, in [8], the linear equalization techniques such as zero forcing (ZF) and minimum mean squared error (MMSE) have been employed to estimate the NCS in the MAC phase by using the sum and difference of the baseband signals coming from the different UEs. After that, these estimates are used to form the log likelihood ratio (LLR) of the NCS, where the LLR consists of the information about the variances on each antenna after the equalization. In [9], the PNC schemes with multiple antennas systems have been extended to the multiuser massive MIMO communication by employing sum and difference matrix concept. In this work, the BER performances of multiuser massive MIMO based PNC have been provided without neither the coverage probability analysis nor closed form expression. The MIMO-PNC systems have been examined through the user-antenna selection and V-BLAST detection in [10], [11]. [12] provided distributed massive MIMO through the performance on the frame error rate. [13] considered the network MIMO by evaluating the performance by using outage probability. [14] focused on throughput and harvested energy for non-orthogonal multiple access (NOMA)-PNC combination.

The coverage analysis of the MIMO systems without considering PNC has been studied in [15]–[17]. Besides, the cellular network analysis based on stochastic geometry have been presented to evaluate coverage in [18]–[20]. For stochastic geometry-based cellular network, the signal-to-interference-plus-noise ratio (SINR) distribution is computed to characterize the coverage probability for the single antenna case in [18] while the MIMO systems have been covered by [19], [20]. Further, the coverage and outage analysis for cellular networks have been presented in [21], [22] considering secrecy and heterogeneity. For the PNC with single antenna case, the coverage probability analysis has been given in [23]. In this paper, we derive the closed form expression of coverage probability for the massive MIMO-PNC by using linear equalization techniques, which has not been covered by the literature to the best knowledge of the authors.

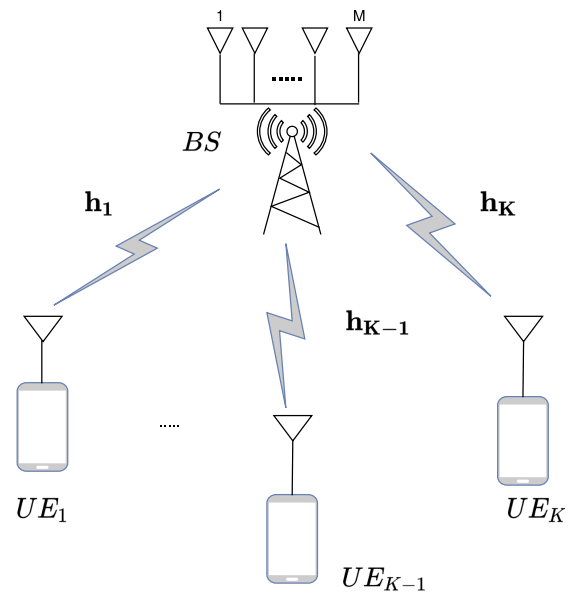


Fig. 1. System Model of PNC based Massive MIMO.

The remainder of this paper is organized as follows. In Section II, we present the system model. Section III proposes the coverage analysis of PNC for the massive MIMO communication systems. The performance results are presented in Section IV. Finally, the conclusions and future research directions are given in Section V.

Notation: Vectors and matrices are given in lower case bold font and upper case bold font, respectively, such as \mathbf{x} and \mathbf{H} . x_{ij} is the j th element of \mathbf{x}_i . $\mathbf{I}_{N \times N}$ represents an identity matrix whose dimension is $N \times N$. $[\mathbf{A}]_{i,j}$ denotes the entry of matrix \mathbf{A} in the i th row and j th column. \mathbf{A}_{ij} denotes the minor of $[\mathbf{A}]_{i,j}$. \mathbf{A}^{sc} denotes the Schur component of \mathbf{A} . $(\cdot)^T$, $(\cdot)^H$, $\mathbb{E}\{\cdot\}$, $tr(\cdot)$ denote the transpose, Hermitian transpose, expectation and trace operators respectively. $\|\cdot\|_F$ denotes the Frobenius norm.

II. SYSTEM MODEL

The considered system model shown in Fig. 1 consists of one BS equipped with M antennas and K UEs each equipped with a single antenna. Each user has a user pair to share their data through the BS by using PNC. Thus, $Q = K/2$ user pairs are formed in the PNC system. It is assumed that users and the BS are perfectly synchronized and all users send their data simultaneously to the BS. In the MAC phase, the aim of the BS is to estimate the NCS belonging to all user pairs. For the BC phase, each NCS is broadcasted to its corresponding pair. Then, each user extracts its pair's data by performing the network coding operation by using its own data and corresponding NCS element.

For MAC phase, the received vector \mathbf{r} at the BS is given as:

$$\mathbf{r} = \mathbf{H}\sqrt{\mathbf{\Gamma}}\mathbf{x} + \mathbf{n} \quad (1)$$

where \mathbf{H} is the composite channel matrix with the dimension of $M \times K$, $\mathbf{\Gamma} = \text{diag}(\Gamma_1, \dots, \Gamma_K)$ includes path loss belonging to all users, $\mathbf{x} = [x_1, x_2, \dots, x_K]^T$ is the composite

transmit symbol vector with a total transmit power constraint $\mathbb{E}\{\|\mathbf{x}\|^2\} \leq P$, \mathbf{n} is the additive white Gaussian noise (AWGN) and modeled by $\mathbf{n} \sim \mathcal{CN}(\mathbf{0}_M, \sigma^2 \mathbf{I}_M)$.

The composite channel matrix \mathbf{H} includes all channel vectors between all UEs and the BS by,

$$\mathbf{H} = \begin{bmatrix} \mathbf{h}_1 & \mathbf{h}_2 & \cdots & \mathbf{h}_K \end{bmatrix} \quad (2)$$

where $\mathbf{h}_k \in \mathbb{C}^{M \times 1}$, $\forall k \in \{1, 2, \dots, K\}$ is the channel vector from k th user to the BS and each of its entries is the complex Gaussian random variable with zero mean and unity variance.

Then, the channel composite matrix holds:

$$\mathbb{E}\{\|\mathbf{H}\|_F^2\} = \text{tr}\{\mathbb{E}\{\mathbf{H}\mathbf{H}^H\}\} = MK \quad (3)$$

For the average received power is given by,

$$\mathbb{E}\{|\sqrt{\Gamma_k} \mathbf{x}_k|^2\} = p_k \quad (4)$$

Then, the averaged received SNR belonging to the k th user is defined by,

$$\gamma_k = \frac{M p_k}{\sigma^2} \quad (5)$$

When the total transmit power is equally shared between the users and their path loss gains are set to unity for the sake of simplicity, the averaged received SNR per user is written as,

$$\gamma_0 = \frac{M P}{K \sigma^2} \quad (6)$$

Before deriving the coverage probability analysis, we give the estimation of the NCS vector for the PNC based MIMO systems by using linear detection techniques [9].

Firstly, the received vector in Eq. (1) can be rewritten as follows [8]:

$$\begin{aligned} \mathbf{r} &= \mathbf{H}\mathbf{D}^{-1}\mathbf{D}\mathbf{x} + \mathbf{n} \\ &= \hat{\mathbf{H}}\hat{\mathbf{x}} + \mathbf{n} \end{aligned} \quad (7)$$

where the reformed composite channel matrix $\hat{\mathbf{H}}$ is represented as follows:

$$\hat{\mathbf{H}} = \mathbf{H}\mathbf{D}^{-1} \quad (8)$$

and the reformed transmitted symbol vector $\hat{\mathbf{x}}$, whose elements are the sums and the differences of the user pairs' transmitted symbols, is given by:

$$\hat{\mathbf{x}} = \mathbf{D}\mathbf{x} \quad (9)$$

with the sum-difference matrix \mathbf{D} is defined as,

$$\mathbf{D} = \begin{bmatrix} \mathbf{I}_{Q \times Q} & \mathbf{I}_{Q \times Q} \\ \mathbf{I}_{Q \times Q} & -\mathbf{I}_{Q \times Q} \end{bmatrix}_{K \times K} \quad (10)$$

Then, $\hat{\mathbf{x}}$ can be written by,

$$\hat{\mathbf{x}} = \begin{bmatrix} x_1 + x_{Q+1} \\ x_2 + x_{Q+2} \\ \vdots \\ x_Q + x_{2Q} \\ x_1 - x_{Q+1} \\ x_2 - x_{Q+2} \\ \vdots \\ x_Q - x_{2Q} \end{bmatrix} \quad (11)$$

With the assumption that the perfect channel state information (CSI) is available at the BS, we perform ZF equalization as follows:

$$\mathbf{G} = (\hat{\mathbf{H}}^H \hat{\mathbf{H}})^{-1} \hat{\mathbf{H}}^H \quad (12)$$

Then, the received signal vector after equalization with the dimension of $2Q \times 1$ is given by:

$$\begin{aligned} \mathbf{y} &= \mathbf{G}\mathbf{r} \\ &= \mathbf{G}\hat{\mathbf{H}}\hat{\mathbf{x}} + \mathbf{G}\mathbf{n} \end{aligned} \quad (13)$$

The noise variances after equalization are defined as σ_q^2 and σ_{q+Q}^2 and then the LLR value [8] belonging to the q th user pair is given in Eq. (14):

$$\begin{aligned} \text{LLR}_q &= \\ &\log \left(\frac{\exp\left(-\frac{2}{\sigma_{q+Q}^2}\right) \left(\exp\left(\frac{2y_{q+Q}}{\sigma_{q+Q}^2}\right) + \exp\left(-\frac{2y_{q+Q}}{\sigma_{q+Q}^2}\right) \right)}{\exp\left(-\frac{2}{\sigma_q^2}\right) \left(\exp\left(\frac{2y_q}{\sigma_q^2}\right) + \exp\left(-\frac{2y_q}{\sigma_q^2}\right) \right)} \right) \end{aligned} \quad (14)$$

The variance of the k th user symbol is calculated by,

$$\sigma_k^2 = \{\mathbf{G}\mathbf{G}^H\}_{k,k} \sigma^2 \quad (15)$$

Then, \mathbf{x}_R is the NCS vector with dimension $Q \times 1$ and is defined by XOR operation as follows:

$$\mathbf{x}_R = \begin{bmatrix} x_{R_1} \\ x_{R_2} \\ \vdots \\ x_{R_Q} \end{bmatrix} = \begin{bmatrix} x_1 \oplus x_{Q+1} \\ x_2 \oplus x_{Q+2} \\ \vdots \\ x_Q \oplus x_{2Q} \end{bmatrix} \quad (16)$$

Finally, the NCS of q th user pair with $\forall q \in \{1, 2, \dots, Q\}$ is determined by [9]:

$$x_{R_q} = \begin{cases} 1 & \text{LLR}_q \geq 0 \\ -1 & \text{otherwise} \end{cases} \quad (17)$$

Finally, the SNR after equalization for the symbol of k th user, whose proof is given in the Appendix A, is written as follows:

$$\rho_k = \frac{2\gamma_0}{\{(\hat{\mathbf{H}}^H \hat{\mathbf{H}})^{-1}\}_{k,k}}, \quad (18)$$

III. COVERAGE ANALYSIS FOR MASSIVE MIMO-PNC

In this section, the coverage probability of PNC in massive MIMO is analyzed. Based on the SNR value after equalization in Eq. (18), the coverage probability for a user pair is defined in the following.

Definition: The coverage probability of a user pair in the massive MIMO-PNC is the probability that the minimum SNR value after equalization for the q th and $(q + Q)$ th symbols are greater than a given threshold τ . Thus, to derive the coverage probability, it is sufficient to check the minimum one with respect to the target value.

$$P_{q,q+Q}^{cov} = \Pr(\min(\rho_q, \rho_{q+Q}) \geq \tau), \forall q \in \{1, 2, \dots, Q\} \quad (19)$$

Then, as it is known, the probability that the minimum of two random variables is greater than a value can be expressed as the joint probability of two events as follows:

$$P_{q,q+Q}^{cov} = \Pr(\rho_q \geq \tau, \rho_{q+Q} \geq \tau), \forall q \in \{1, 2, \dots, Q\} \quad (20)$$

Since two events in Eq. (20), are independent from each other, we can define coverage probability as the multiplication of the separate events and it can be expressed for the q th symbol with $q = 1, 2, \dots, Q$:

$$P_{q,q+Q}^{cov} = \Pr(\rho_q \geq \tau) \Pr(\rho_{q+Q} \geq \tau) \quad (21)$$

In order to derive the coverage probability of massive MIMO-PNC in the closed form, probability density function (PDF) of the SNR after equalization is required.

Theorem: The SNR value after ZF equalization obtained through sum difference matrix is gamma distributed and its PDF for the k th user is defined as follows:

$$f_{P_k}(\rho_k) = \frac{1}{\gamma_0(M-K)!} e^{-\left(\frac{\rho_k}{\gamma_0}\right)} \left(\frac{\rho_k}{\gamma_0}\right)^{M-K}, \quad (22)$$

The proof of the Theorem is given in the Appendix B.

The rate parameter is given by $\beta = \frac{1}{\gamma_0}$ while $\alpha = M - K + 1$ is defined as the shape parameter.

After defining these two parameters, Eq. (22) can be rewritten as follows:

$$f_{P_k}(\rho_k) = \frac{\beta^\alpha}{\Gamma(\alpha)} e^{-(\beta\rho_k)} \rho_k^{\alpha-1} \quad (23)$$

where $\Gamma(\cdot)$ is the gamma function which is defined as follows:

$$\Gamma(\alpha) = \int_0^\infty x^{\alpha-1} e^{-x} dx. \quad (24)$$

Further, Eq. (21) can be rewritten knowing that the probability that a random variable lies in a specific interval is the integral of its PDF over this interval as follows:

$$P_{q,q+Q}^{cov} = \int_\tau^\infty f_{P_q}(\rho_q) d\rho_q \int_\tau^\infty f_{P_{q+Q}}(\rho_{q+Q}) d\rho_{q+Q} \quad (25)$$

In order to achieve the closed form of the coverage probability, the integral terms can be replaced with the complementary cumulative distribution function (CCDF) of the SNR after the

TABLE I
SIMULATION PARAMETERS

Parameters	Values
No. antennas at the BS, M	4,8,16,30,32,60,100,120
No. UEs, K	2,4,20,40,60
No. antennas per UE	1
SNR (dB)	0, 5, 10, 20
Channel \mathbf{H} ,	i.i.d. Rayleigh
No iteration	5×10^4
Linear Detector	ZF

equalization as follows:

$$P_{q,q+Q}^{cov} = (1 - F_{P_q}(\tau))(1 - F_{P_{q+Q}}(\tau)) \quad (26)$$

where F_{P_k} is the cumulative distribution function (CDF) of the SNR value after equalization which can be given as follows:

$$F_{P_k}(\rho_k) = \int_0^{\rho_k} f_{P_k}(u; \beta, \alpha) du = \frac{\gamma(\alpha, \beta\rho_k)}{\Gamma(\alpha)} \quad (27)$$

where $\gamma(\cdot, \cdot)$ is the lower incomplete gamma function which is given as follows:

$$\gamma(\alpha, \beta\rho_k) = \int_0^{\beta\rho_k} t^{\alpha-1} e^{-t} dt. \quad (28)$$

Then, Eq. (26) can be expressed as:

$$P_{q,q+Q}^{cov} = \left(1 - \frac{\gamma(\alpha, \beta\tau)}{\Gamma(\alpha)}\right) \left(1 - \frac{\gamma(\alpha, \beta\tau)}{\Gamma(\alpha)}\right) \quad (29)$$

Note that, for both q th and $(q + Q)$ th equalized SNR, the parameters β and α for CDF calculation are the same. Finally, the coverage probability of the PNC for a user pair is obtained as follows:

$$P_{q,q+Q}^{cov} = \left(1 - \frac{\gamma(\alpha, \beta\tau)}{\Gamma(\alpha)}\right)^2 \quad (30)$$

The average coverage probability of the PNC for Q user pairs is given as follows:

$$\overline{P}^{cov} = \frac{1}{Q} \sum_{q=1}^Q P_{q,q+Q}^{cov}. \quad (31)$$

The derivations can be provided by considering Eq. (5) by replacing γ_0 to γ_k and β to β_k .

IV. PERFORMANCE RESULTS

In this section, we illustrate the theoretical and simulation results for different number of users in the MIMO-PNC systems having moderate to massive number of antennas at the BS. The simulation parameters are listed in Table I.

While providing the performance results, for each iteration, the SNR values after equalization are determined as in Eq. (18) based on the composite channel matrix generated through Rayleigh fading. Then, the user pairs that have higher SNR after equalization value than a given target SNR are counted. Finally, these results are averaged through different channel realizations. For the theoretical results, the coverage probability for each user pair is directly calculated by using Eq. (30) based on the average

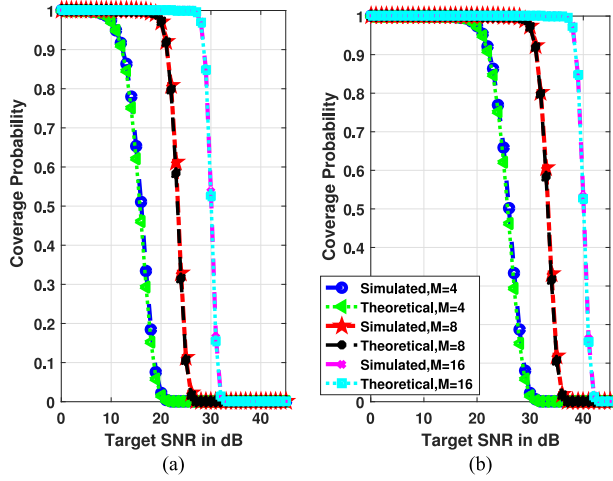


Fig. 2. Coverage probability vs different number of antennas at the BS in the massive MIMO-PNC for $K = 2$ when the average user SNR is (a) 10 dB (b) 20 dB.

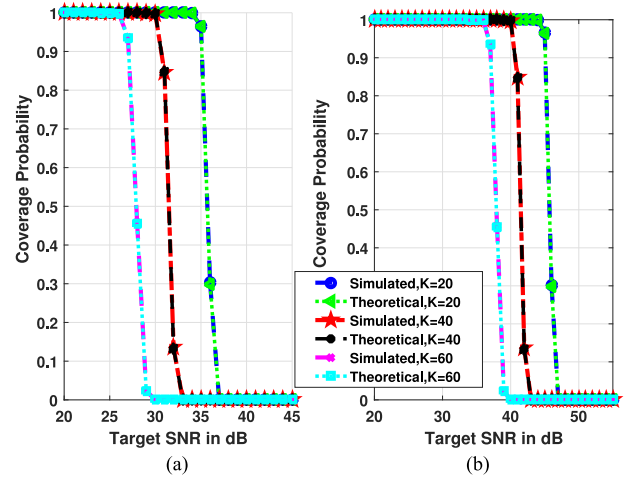


Fig. 4. Coverage probability vs different number of antennas at the BS in the massive MIMO-PNC for $M = 100$ when the average user SNR is (a) 10 dB (b) 20 dB.

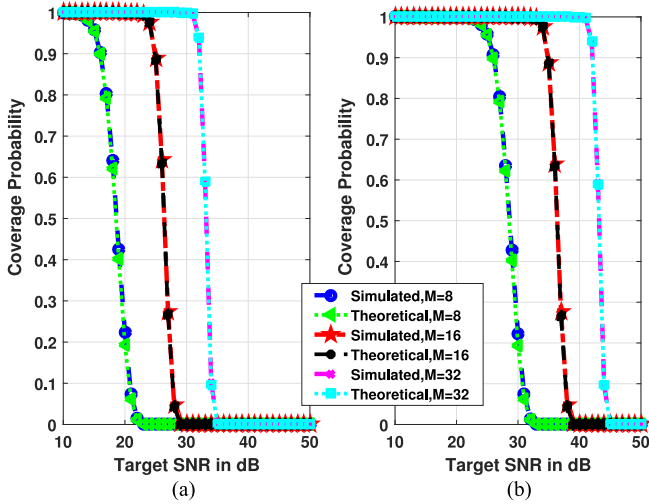


Fig. 3. Coverage probability vs different number of antennas at the BS in the massive MIMO-PNC for $K = 4$ when the average user SNR is (a) 10 dB (b) 20 dB.

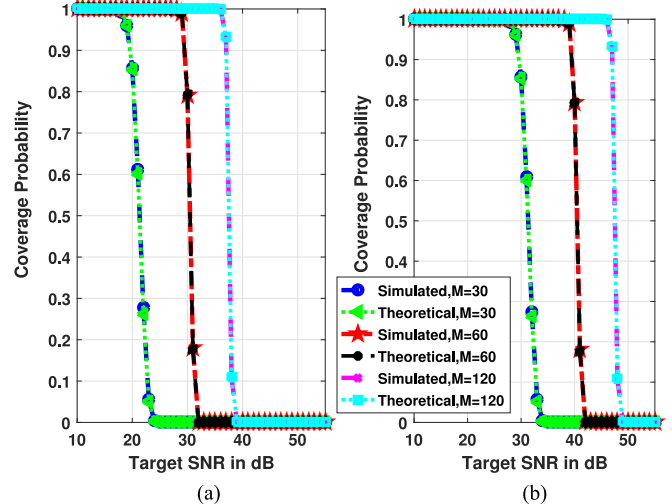


Fig. 5. Coverage probability vs different number of antennas at the BS in the massive MIMO-PNC for $K = 20$ when the average user SNR is (a) 10 dB (b) 20 dB.

SNR value for each user γ_0 , a given target SNR value τ , the number of users K , and the number of the antennas at the BS, M . Then, these results are averaged for Q user pairs as given in Eq. (31).

In the Figs. 2 and 3, the theoretical and simulation results of the coverage probability for different number of antennas at the BS are provided for the case of $K = 2$ and $K = 4$ users respectively when the average user SNR values are 10 dB and 20 dB. It is shown that the coverage probability is increased proportional to the number of antennas at the BS when the number of users is fixed. Besides, the coverage probability is reduced when the number of users is increased for a fixed number of antennas.

In the Figs. 4 and 5, the theoretical and simulation results of the coverage probability are demonstrated in the massive MIMO systems for different number of antennas at the BS and different users deployment when the average received SNR values are 10 dB and 20 dB. According to the results, the coverage probability is significantly increased by the number

of antennas at the BS while supporting high number of users. In addition to that the coverage probability is also improved when the received SNR is increased from 10 dB to 20 dB in the massive MIMO systems. Besides, it is demonstrated that even the average user SNR is less than a target SNR value, the BS can cover all the users with the calculation of the NCS due to the performance enhancement of the massive MIMO-PNC through ZF equalization. Specifically, the received SNR is improved up to 25 dB while satisfying the coverage of 90% for the systems with $M = 100$ and $K = 20$ as in Fig. 4.

In the Figs. 6 and 7, the theoretical and simulation results of the coverage probability are demonstrated by considering low user SNR values as 0 dB and 5 dB, respectively. In these Figures, the applicability of PNC-MIMO systems is also demonstrated in the low SNR regimes while preserving the same SNR improvement as in the high SNR regimes.

In the Figs. 8 and 9, theoretical and simulation results of the coverage probability for different number of users and different

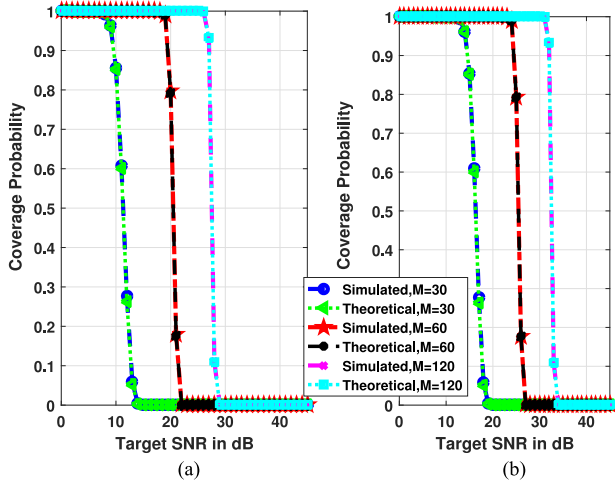


Fig. 6. Coverage probability vs different number of antennas at the BS in the massive MIMO-PNC for $K = 20$ when the average user SNR is (a) 0 dB (b) 5 dB.

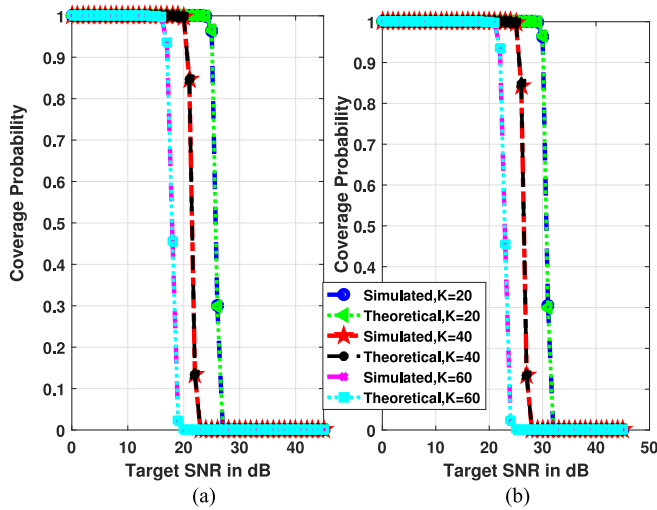


Fig. 7. Coverage probability vs different number of antennas at the BS in the massive MIMO-PNC for $M = 100$ when the average user SNR is (a) 0 dB (b) 5 dB.

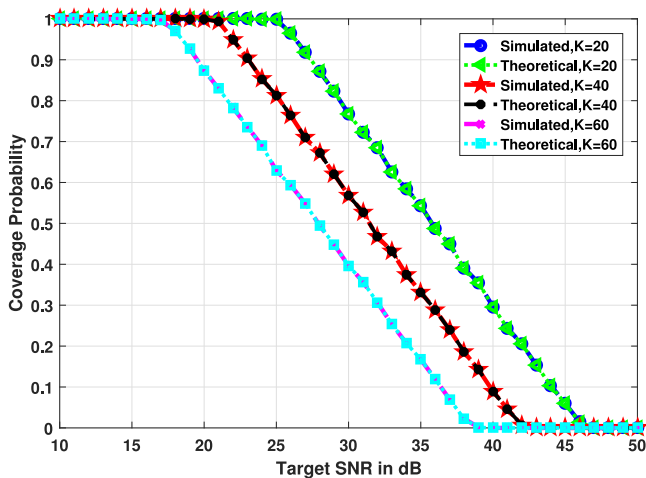


Fig. 8. Coverage probability vs different number of users in the massive MIMO-PNC for $M = 100$ when the user SNR is uniformly distributed between 0 dB and 20 dB.

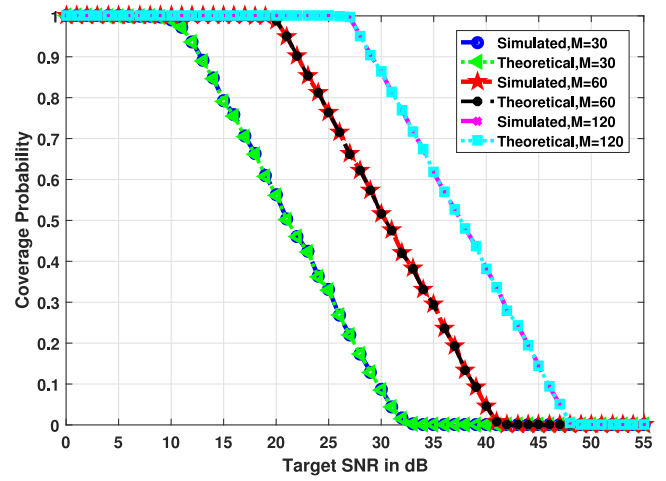


Fig. 9. Coverage probability vs different number of antenna at BS in the massive MIMO-PNC with $K = 20$ when the user SNR is uniformly distributed between 0 dB and 20 dB.

number of antennas at the BS are provided when the user SNR values are uniformly distributed between 0 – 20 dB respectively. As shown in Fig. 8, as the number of users decreases for a fixed number of antennas at the BS, the performance of coverage probability is improved remarkably. As shown in Fig. 9, the massive MIMO has improved the coverage probability proportional to the number of antennas at the BS for the PNC based massive MIMO systems.

V. CONCLUSION

In this paper, the coverage probability of PNC in massive MIMO systems have been examined. The closed form of coverage probability is derived based on the distribution of SNR after equalization in the PNC based systems with ZF equalization. We have demonstrated that the theoretical and simulation results are perfectly matched in the massive MIMO-PNC systems with different number of users and antennas at the BS. It has been shown that the BS can serve all users through the massive MIMO-PNC with ZF equalization even when the average SNR values of the user pairs are low. We have also shown the massive MIMO provides a significant gain on the coverage compared to MIMO systems for the PNC based communications. The proposed coverage analysis can be extended to the multi-cell massive MIMO-PNC by using stochastic geometry in unsuper-vised networks.

APPENDIX

A. Proof of 18

By using the expression of the equalized received signal given in Eq. (13) and knowing that $\mathbb{E}\{\|\mathbf{G}\hat{\mathbf{H}}\|_F^2\} = M$, the SNR after equalization for k th estimated symbol can be defined as follows:

$$\rho_k = \frac{M[\mathbb{E}\{\hat{\mathbf{x}}\hat{\mathbf{x}}^H\}]_{k,k}}{[\mathbb{E}\{\mathbf{G}\mathbf{n}\mathbf{n}^H\mathbf{G}^H|\mathbf{H}\}]_{k,k}} \quad (32)$$

Then $\hat{\mathbf{x}}$ is expanded as follows:

$$\rho_k = \frac{M[\mathbb{E}\{\mathbf{D}\mathbf{x}\mathbf{x}^H\mathbf{D}\}]_{k,k}}{[\mathbb{E}\{\mathbf{G}\mathbf{m}\mathbf{m}^H\mathbf{G}^H|\mathbf{H}\}]_{k,k}} \quad (33)$$

Since \mathbf{D} is a deterministic matrix, it can be taken out from the expectation operator as follows:

$$\rho_k = \frac{M[\mathbf{D}\mathbb{E}\{\mathbf{x}\mathbf{x}^H\}\mathbf{D}^H]_{k,k}}{[\mathbb{E}\{\mathbf{G}\mathbf{m}\mathbf{m}^H\mathbf{G}^H|\mathbf{H}\}]_{k,k}} \quad (34)$$

By using the constraint on the power, the numerator is revised as follows:

$$\rho_k = \frac{M(P/K)[\mathbf{D}\mathbf{I}\mathbf{D}^H]_{k,k}}{[\mathbb{E}\{\mathbf{G}\mathbf{m}\mathbf{m}^H\mathbf{G}^H|\mathbf{H}\}]_{k,k}} \quad (35)$$

Since $\mathbf{D}\mathbf{D}^H = 2\mathbf{I}$, the final expression for the numerator is obtained as,

$$\rho_k = \frac{2M(P/K)}{[\mathbb{E}\{\mathbf{G}\mathbf{m}\mathbf{m}^H\mathbf{G}^H|\mathbf{H}\}]_{k,k}} \quad (36)$$

Knowing that the conditional expectation conditioning on \mathbf{H} is taken, \mathbf{G} is not random for this expectation and can be taken out from the expectation operator as follows:

$$\rho_k = \frac{2M(P/K)}{[\mathbf{G}\mathbb{E}\{\mathbf{m}\mathbf{m}^H\}\mathbf{G}^H]_{k,k}} \quad (37)$$

After the replacement of the auto covariance matrix of the noise vector, the expression above becomes:

$$\rho_k = \frac{2MP}{K\sigma^2[\mathbf{G}\mathbf{G}^H]_{k,k}} \quad (38)$$

Finally, knowing that $\mathbf{G}\mathbf{G}^H = (\hat{\mathbf{H}}^H\hat{\mathbf{H}})^{-1}$ and using Eq. (6), the expression for ρ_k is obtained as follows:

$$\rho_k = \frac{2\gamma_0}{[(\hat{\mathbf{H}}^H\hat{\mathbf{H}})^{-1}]_{k,k}} \quad (39)$$

B. Proof of 22

In [24], it is given that $2\mathbf{H}^H\mathbf{H}$ term is complex Wishart matrix. Then, we can define a complex Wishart matrix $\hat{\mathbf{Z}}$ which is formed from the manipulated channel matrix in Eq. (2) as follows:

$$\hat{\mathbf{Z}} = 2\hat{\mathbf{H}}^H\hat{\mathbf{H}}. \quad (40)$$

Then, the distribution of $\hat{\mathbf{Z}}$ can be defined as follows:

$$\mathbf{W}_M(K, \hat{\mathbf{\Sigma}}) = \frac{e^{\text{tr}(-\hat{\mathbf{\Sigma}}^{-1}\hat{\mathbf{Z}})}|\hat{\mathbf{Z}}|^{(M-K)}}{\Gamma_M(K)|\hat{\mathbf{\Sigma}}|^M} \quad (41)$$

where $\hat{\mathbf{\Sigma}}$ is the scale matrix of $\hat{\mathbf{Z}}$ and $\Gamma_M(\cdot)$ is the M -variate complex multivariate gamma function.

Next, using Eq. (40), Eq. (18) can be arranged as follows:

$$\rho_k = \gamma_0 \frac{1}{[(\hat{\mathbf{Z}})^{-1}]_{k,k}} \quad (42)$$

Further, Eq. (42) is re-written by the inverse matrix definition as follows:

$$\rho_k = \gamma_0 \frac{|\hat{\mathbf{Z}}|}{|\hat{\mathbf{Z}}_{k,k}|} \quad (43)$$

Using the fact $|\hat{\mathbf{Z}}| = |\hat{\mathbf{Z}}_{k,k}||\hat{\mathbf{Z}}_{k,k}^{sc}|$, Eq. (43) can be written as follows:

$$\rho_k = \gamma_0 |\hat{\mathbf{Z}}_{k,k}^{sc}| \quad (44)$$

$\hat{\mathbf{Z}}_{k,k}^{sc}$ can be also defined as a Wishart matrix distributed as $\mathbf{W}_1(M-K+1, \hat{\mathbf{\Sigma}}_{kk}^{sc})$. In other word, $s = |\hat{\mathbf{Z}}_{k,k}^{sc}|$ is a Chi squared random variable where its PDF given as:

$$f_S(s) = \frac{e^{-\frac{s}{\hat{\mathbf{\Sigma}}_{kk}^{sc}}}}{\hat{\mathbf{\Sigma}}_{kk}^{sc}(M-K)!} \left(\frac{s}{\hat{\mathbf{\Sigma}}_{kk}^{sc}}\right)^{(M-K)} \quad (45)$$

Further, from Eq. (44), the following change of variable is used to find the PDF of ρ_k as $s = |\hat{\mathbf{Z}}_{k,k}^{sc}| = \frac{\rho_k}{\gamma_0}$. Since Schur complement of the minor is a scalar, its determinant becomes itself $s = \hat{\mathbf{Z}}_{k,k}^{sc} = \frac{\rho_k}{\gamma_0}$. Because change of variable to Chi squared variable s is made, its corresponding scale matrix must be changed from $\hat{\mathbf{\Sigma}}_{kk}^{sc}$ to $\gamma_0 \hat{\mathbf{\Sigma}}_{kk}^{sc}$. Then, Eq. (45) becomes:

$$f_S\left(\frac{\rho_k}{\gamma_0}\right) = \frac{e^{-\frac{\rho_k}{\gamma_0^2 \hat{\mathbf{\Sigma}}_{kk}^{sc}}}}{\gamma_0 \hat{\mathbf{\Sigma}}_{kk}^{sc}(M-K)!} \left(\frac{\rho_k}{\gamma_0^2 \hat{\mathbf{\Sigma}}_{kk}^{sc}}\right)^{(M-K)} \quad (46)$$

Note that in the argument of the function in Eq. (46), we have $\frac{\rho_k}{\gamma_0}$. Then, this function does not stand for the PDF of ρ_k . In order to obtain PDF, ρ_k must be replaced with $\rho_k \gamma_0$ as follows:

$$f_{P_k}(\rho_k) = \frac{e^{-\frac{\rho_k}{\gamma_0 \hat{\mathbf{\Sigma}}_{kk}^{sc}}}}{\gamma_0 \hat{\mathbf{\Sigma}}_{kk}^{sc}(M-K)!} \left(\frac{\rho_k}{\gamma_0 \hat{\mathbf{\Sigma}}_{kk}^{sc}}\right)^{(M-K)} \quad (47)$$

It is known that $\hat{\mathbf{\Sigma}}_{kk}^{sc} = \frac{1}{[(\hat{\mathbf{\Sigma}})^{-1}]_{kk}}$. After, since the first moment of the Wishart matrix $\hat{\mathbf{Z}}$ is the multiplication of its scale matrix $\hat{\mathbf{\Sigma}}$ with its degree of the freedom M , the scale matrix can be obtained by

$$\begin{aligned} \hat{\mathbf{\Sigma}} &= \frac{1}{M} \mathbb{E}\{\hat{\mathbf{Z}}\} \\ &= \frac{2}{M} \mathbb{E}\{\hat{\mathbf{H}}^H\hat{\mathbf{H}}\} \\ &= \frac{2}{M} \mathbb{E}\{(\mathbf{H}\mathbf{D}^{-1})^H\mathbf{H}\mathbf{D}^{-1}\} \\ &= \frac{2}{M} \mathbf{D}^{-1} \mathbb{E}\{\mathbf{H}^H\mathbf{H}\} \mathbf{D}^{-1} \end{aligned} \quad (48)$$

Knowing that $\mathbb{E}\{\mathbf{H}^H\mathbf{H}\} = M\mathbf{I}$ by Eq. (3), and knowing also that $\mathbf{D}^{-2} = \frac{1}{2}\mathbf{I}$, the scale matrix can be found as $\hat{\mathbf{\Sigma}} = \mathbf{I}$. Then, $\hat{\mathbf{\Sigma}}_{kk}^{sc}$ is calculated as 1. Finally, after the replacement of $\hat{\mathbf{\Sigma}}_{kk}^{sc}$ into Eq. (47), Eq. (22) is obtained as follows:

$$f_{P_k}(\rho_k) = \frac{1}{\gamma_0(M-K)!} e^{-\left(\frac{\rho_k}{\gamma_0}\right)} \left(\frac{\rho_k}{\gamma_0}\right)^{(M-K)} \quad (49)$$

REFERENCES

- [1] P. Chen, Z. Xie, Y. Fang, Z. Chen, S. Mumtaz, and J. J. P. C. Rodrigues, "Physical-layer network coding: An efficient technique for wireless communications," *IEEE Netw.*, vol. 34, no. 2, pp. 270–276, Mar./Apr. 2020.
- [2] J. Sykora and A. Burr, *Wireless Physical Layer Network Coding*. Cambridge, U.K.: Cambridge Univ. Press, 2018.
- [3] S. Zhang, S. C. Liew, and P. P. Lam, "Physical-layer network coding," in *Proc. 12th Annu. Int. Conf. Mobile Comput. Netw.*, New York, NY, USA, Sep. 2006, pp. 358–365.
- [4] R. H. Y. Louie, Y. Li, and B. Vucetic, "Performance analysis of physical layer network coding in two-way relay channels," in *Proc. IEEE Glob. Telecommun. Conf.*, Honolulu, HI, USA, Nov. 2009, pp. 1–6.
- [5] M. Lu, Z. Shen, D. Guo, and X. Wang, "A new physical layer network coding de-noising mapping based on M-QAM," in *Proc. First Int. Conf. Electron. Instrum. Inf. Syst.*, Harbin, China, Jun. 2017, pp. 1–5.
- [6] V. Nambodiri, K. Venugopal, and B. Rajan, "Physical layer network coding for two-way relaying with QAM," *IEEE Trans. Wireless Commun.*, vol. 12, no. 10, pp. 5074–5086, Oct. 2013.
- [7] K. Lu, S. Fu, Y. Qian, and H. Chen, "SER performance analysis for physical layer network coding over AWGN channels," in *Proc. IEEE Glob. Telecommun. Conf.*, Honolulu, HI, USA, Nov. 2009, pp. 1–6.
- [8] S. Zhang and S. C. Liew, "Physical layer network coding with multiple antennas," in *Proc. IEEE Wireless Commun. Netw. Conf.*, Sydney, Australia, Apr. 2010, pp. 1–6.
- [9] B. Okyere, L. Musavian, and R. Mumtaz, "Multi-user massive MIMO and physical layer network coding," in *Proc. IEEE Glob. Commun. Conf. Workshops.*, Waikoloa, HI, USA, Dec. 2019, pp. 1–6.
- [10] V. Kumar, B. Cardiff, and M. Flanagan, "User-antenna selection for physical-layer network coding based on euclidean distance," *IEEE Trans. Commun.*, vol. 67, no. 5, pp. 3363–3375, May. 2019.
- [11] Y. Li, S. Zhang, and H. Wang, "BER performance analysis of MIMO physical-layer network coding based on VBLAST detection," in *Proc. IEEE/CIC Int. Conf. Commun. China-Workshops.*, Xi'an, China, Aug. 2013, pp. 170–175.
- [12] A. Burr and D. Fang, "Physical layer network coding for distributed massive MIMO," in *Proc. WSA 19th Int. ITG Workshop Smart Antennas*, Ilmenau, Germany, 2015, pp. 1–5.
- [13] T. Peng, Y. Wang, A. G. Burr, and M. R. Shikh-Bahaei, "Physical layer network coding in network MIMO: A new design for 5G and beyond," *IEEE Trans. Commun.*, vol. 67, no. 3, pp. 2024–2035, Mar. 2019.
- [14] S. Khosroozad, S. Naderi, and A. Abedi, "Using physical layer network coding to improve NOMA system throughput with energy harvesting users," in *Proc. IEEE Glob. Commun. Conf.*, Waikoloa, HI, USA, 2019, pp. 1–6.
- [15] B. Razeghi, G. Hodtani, and S. Seyedin, "Coverage region analysis for MIMO amplify-and-forward relay channel with the source to destination link," in *Proc. 7th Int. Symp. Telecommun.*, Tehran, Iran, Sep. 2014, pp. 1133–1137.
- [16] S. Kumar, S. Kalyani, L. Hanzo, and K. Giridhar, "Coverage probability and achievable rate analysis of FFR-Aided multi-user OFDM-Based MIMO and SIMO systems," *IEEE Trans. Commun.*, vol. 63, no. 10, pp. 3869–3881, Oct. 2015.
- [17] M. Khoshkholgh, K. Navaie, K. Shin, and V. Leung, "Coverage analysis of multi-stream MIMO hetnets with MRC receivers," vol. 16, no. 12, pp. 7816–7833, Dec. 2017.
- [18] J. G. Andrews, A. K. Gupta, and H. S. Dhillon, "A primer on cellular network analysis using stochastic geometry," *CoRR*, Apr. 2016, *arXiv:1604.03183*. [Online]. Available: <http://arxiv.org/abs/1604.03183>
- [19] P. Parida and H. Dhillon, "Stochastic geometry-based uplink analysis of massive MIMO systems with fractional pilot reuse," *IEEE Trans. Wireless Commun.*, vol. 18, no. 3, pp. 1651–1668, Mar. 2019.
- [20] M. Null, D. Renzo, and P. Guan, "A mathematical framework to the computation of the error probability of downlink MIMO cellular networks by using stochastic geometry," *IEEE Trans. Commun.*, vol. 62, no. 8, pp. 2860–2879, Aug. 2014.
- [21] S. Monhof, S. Bocker, J. Tiemann, and C. Wietfeld, "Cellular network coverage analysis and optimization in challenging smart grid environments," in *Proc. IEEE Int. Conf. Commun., Control, Comput. Technol. Smart Grids*, Aalborg, Denmark, Oct. 2018, pp. 1–6.
- [22] Y. Panziyu and H. Baoziyong, "Approximate coverage analysis of heterogeneous cellular networks modeled by poisson hole process," in *Proc. IEEE 18th Int. Conf. Commun. Technol.*, Chongqing, China, Oct. 2018, pp. 424–427.
- [23] H. Fukui, P. Popovski, and H. Yomo, "Physical layer network coding: An outage analysis in cellular network," in *Proc. 22nd Eur. Signal Process. Conf.*, Lisbon, Portugal, Nov. 2014, pp. 1133–1137.
- [24] D. Gore, R. Heath, and A. Paulraj, "On performance of the zero forcing receiver in presence of transmit correlation," in *Proc. IEEE Int. Symp. Inf. Theory*, Lausanne, Switzerland, 2002, p. 159.



Mert İlgüy received the B.Sc. degree with a first rank in electronics and communication engineering in 2018 and the M.Sc. degree in telecommunication field in 2021 from the İzmir Institute of Technology, Urla, Turkey, where he is currently working toward the Ph.D. degree. In 2019, he was a Research Assistant with the İzmir Institute of Technology. His research interests include physical layer network coding, massive MIMO, and NOMA systems.



Berna Özbek is currently an Associate Professor in telecommunication field with Electrical and Electronics Engineering Department, İzmir Institute of Technology, Urla, Turkey, and is working in the field of wireless communication systems for more than 15 years. She has been awarded as a Marie-Curie Intra-European (EIF) Fellowship by the European Commission for two years. She has coordinated one international and four national projects, was a consultant for three Eureka-Celtic projects, and three national industry-driven projects. Under her supervision, 14 master' thesis and two doctoral dissertations have been completed. She is currently supervising three Ph.D. and one master' students and conducting one national and one international project. She has authored or coauthored more than 90 peer-reviewed papers, one book, one book chapter, and two patents. Her research interests include interference management, resource allocation, limited feedback links, device-to-device communications, physical layer security, massive MIMO systems, and mmwave communications.



Rao Mumtaz received the M.Sc. degree from the Blekinge Institute of Technology, Karlskrona, Sweden, in 2011 and the Doctoral degree in 2016. He has more than 12 years of R&D experience in the wireless communications industry, working with Ericsson, IT, Huawei Research Labs, and GS-LDA. His research interests include 5G radio communication protocols and architectures, and quantum communications.



Sherif A. Busari (Member, IEEE) received the B.Eng. and M.Eng. degrees in electrical and electronics engineering from the Federal University of Technology Akure, Akure, Nigeria, in 2011 and 2015, respectively, and an industry-driven Ph.D. degree in telecommunications engineering from the Universidade de Aveiro, Aveiro, Portugal, in 2020. His research interests include technology enablers and system level simulation methodologies for 5G and beyond-5G networks.



Jonathan Gonzalez received the M.Sc. and Ph.D. degrees in telecommunications from the University of Surrey, Guildford, U.K., in 1999 and 2004, respectively. He was a Senior Researcher with the University of Surrey, where he was responsible for project development and research on mobile systems. In 2019, he was an Honorary Senior Researcher with the University of Bradford, Bradford, U.K. In 2011, he founded GS-LDA-Portugal, targeting R&I on next generation mobile platforms. He has more than 15 years of R&D experience in mobile communications and practical experimentation. His research interests include simulation methodologies, and radio resource management.